Neural Comput & Applic (2017) 28:3903–3920
DOI 10.1007/s00521-016-2296-6

ORIGINAL ARTICLE

An intelligent decision support system for the detection of meat spoilage using multispectral images

Abeer Alshejari[1] · **Vassilis S. Kodogiannis**[1]

Received: 7 November 2015 / Accepted: 30 March 2016 / Published online: 7 April 2016

Abstract In food industry, quality and safety are considered important issues worldwide that are directly related to health and social progress. The use of vision technology for quality testing of food production has the obvious advantage of being able to continuously monitor a production using non-destructive methods, thus increasing the quality and minimizing cost. The performance of an intelligent decision support system has been evaluated in monitoring the spoilage of minced beef stored either aerobically or under modified atmosphere packaging, at different storage temperatures (0, 5, 10, and 15 °C) utilising multispectral imaging information. This paper utilises a neuro-fuzzy model which incorporates a clustering preprocessing stage for the definition of fuzzy rules, while its final fuzzy rule base is determined by competitive learning. Initially, meat samples are classified according to their storage conditions, while identification models are then utilised for the prediction of the Total Viable Counts of bacteria. The innovation of the proposed approach is further extended to the identification of the temperature used for storage, utilizing only imaging spectral information. Results indicated that spectral information in combination with the proposed modelling scheme could be considered as an alternative methodology for the accurate evaluation of meat spoilage.

✉ Vassilis S. Kodogiannis
V.Kodogiannis@westminster.ac.uk

Abeer Alshejari
a.alshejari@my.westminster.ac.uk

[1] Faculty of Science and Technology, University of Westminster, London W1W 6UW, UK

Keywords Neurofuzzy systems · Modelling · Classification · Meat spoilage · Neural networks · Regression

1 Introduction

With the current growing need for lower production costs and high competence, food industry is faced with a number of challenges, including maintenance and assurance of food quality and safety. Food companies and suppliers need efficient, low-cost and non-invasive quality and safety inspection technologies to enable them to satisfy different markets' needs [1]. Various rapid, non-invasive methods based on analytical instrumental techniques, such as Fourier transform infrared spectroscopy (FTIR) [2], Raman spectroscopy [3] and Electronic Nose technology [4] have been investigated for their potential in assessing food quality. With recent advances in sensorial developments, there have been significant progresses in techniques for assessment of food quality and safety. Machine vision techniques based on RGB colour systems have been successfully applied to the evaluation of foods' external characteristics. Such methods, however, are not able to capture broad spectral information which is related to internal characteristics [5]. The association between NIR spectra and food components makes NIR spectroscopy more attractive than other spectroscopic techniques. Nevertheless, these spectral methods have been proved ineffective to heterogeneous materials such as meat, due to the fact that they are not capable of obtaining any spatial information about objects [6]. In recent years, spectral imaging (i.e. hyperspectral and multispectral) has been considered as an alternative tool for safety and quality inspection of various agricultural products. This technique

integrates the conventional imaging and spectroscopy technique to attain simultaneously both spatial and spectral information from the target product. Inspection of internal and external features in various fruits and vegetables such as apple [7] and fresh-cut spinach leaves [8] have been performed using multispectral imaging combined with various chemometric methods.

Meat is a nutritious and expensive food product in human diet worldwide due to the fact that it is an important source of protein and trace elements. A non-invasive method based on multispectral imaging in the visible and near infrared (NIR) regions to predict the aerobic plate count in cooked pork sausages has been considered recently [9]. The prediction of total viable counts of minced pork meat stored under two different storage conditions—aerobic and modified atmosphere packages—has been performed using the VideometerLab multispectral imaging device [10]. A hyperspectral imaging technique has been investigated for evaluating pork meat tenderness and *Escherichia coli* contamination [11]. In that research study, a Modified Gompertz function was exploited to extract the scattering characteristics of pork meat from the spatially-resolved hyperspectral images. The identification and extraction of useful colour and texture features from fresh beef samples using a multispectral imaging system has been also explored and a support vector machine algorithm was utilised to predict cooked beef tenderness [12]. The detection of minced lamb and minced beef adulteration has been considered using hyperspectral imaging [13, 14], while the possibility of combining both spectral with texture features in order to improve pH prediction for salted pork was investigated through hyperspectral imaging [15].

Application of hyperspectral imaging actually may be restricted due to the resulting large and computationally excessive hypercube. Thus, it is essential to extract characteristic features by operating quantitative analysis [16]. This has been achieved through the integration of modern analytical platforms with computational and chemometric techniques. For quantitative analysis prediction, multivariate analytical tools such as principal component analysis (PCA), partial least square regression (PLS) are widely used modelling methods [17]. However meat spoilage is a dynamic process which leads to the undesirable change in external attributes (colour, texture, and even flavour) as well as to the internal attributes (chemical compositions, tissue structure) of meat. The spectra extracted from hypercube can express the internal changes of meat attributes, and the relationship between meat spoilage and extracted information is very complicated and tends to nonlinearity [18]. Neural networks utilising the back-propagation algorithm (MLP), which is one of the most commonly used non-linear regression method, have been recently used in food applications of hyperspectral imaging [19].

Neural networks (NNs) have become a popular tool in non-parametric function learning due to their ability to learn rather complicated functions. While they have gained much interest in predictive engineering and quantitative modelling, their application in the field of food science is still in its early development stage [20]. NNs usually require a large number of neurons for solving the majority of approximation problems, while the greedy nature of the Gradient Descent (back-propagation) algorithm used in the training process, often settles in undesirable local minima of the error surface or converges too slowly [21]. In addition, NNs are prone to dimensionality problems, as each single neuron-node cannot define a multi-dimensional hyper-sphere of the input domain. Although fuzzy logic systems, provide such input space mapping, they do not have learning ability, thus it is difficult to analyse complex systems without prior and accurate knowledge on the system being analysed [22]. To overcome these limitations of NNs and fuzzy systems, neuro-fuzzy approaches have attracted growing interest of researchers in various scientific and engineering areas.

The main objective of this paper is to associate, for the first time according to literature, spectral data acquired by multispectral imaging techniques with meat spoilage, using neuro-fuzzy systems. An intelligent decision support system initially classifies minced beef samples stored either aerobically or under modified atmosphere packaging and then predicts for each case, the total viable counts (TVC) of bacteria. The Adaptive Fuzzy Inference Neural Network (AFINN), a Takagi–Sugeno–Kang (TSK) based structure, has been considered as the core component for the proposed intelligent decision support system [23]. Results from AFINN scheme are compared against models based on Adaptive Neural Fuzzy Inference System (ANFIS), multilayer neural networks (MLP), as well as non-linear and linear (PLS) regression schemes. Such comparison is considered as a essential test, as we have to emphasise the need of induction to the area of food microbiology, advanced learning-based modelling schemes, which may have a significant potential for the accurate estimation of meat spoilage.

2 Experimental case

2.1 Sample preparation and microbiological analysis

The entire experimental case study was performed at the Agricultural University of Athens, Greece. Minced Meat was separated into small portions (75 g) and packaged

individually either aerobically or under modified atmosphere (MAP) (40 % CO_2, 30 % O_2, 30 % N_2), and in different temperatures (0, 5, 10, 15 °C) that are associated with acceptable/non-acceptable storage practices in a distribution chain for meat products [24]. At the beginning and during storage, after appropriate time intervals, meat samples were divided into two parts; one part was used for microbiological analysis while the other one for image analysis. It was assumed that the microbial population at both parts would be comparable. Aerobic samples stored at 0 and 5 °C were analysed approx. every 48 h for the period 0–186 h and every 24 h for the period 186–378 h. Finally, the last sample was analysed at 479 h. Similarly, samples stored at 10 and 15 °C were analysed approx. every 12 h for the period 0–156 h. In total, 14 samples were analysed for each temperature case, resulting 56 samples in total. The same procedure was repeated for MAP case too. Microbiological analysis was performed, and resulting growth data from plate counts were $\log_{10}$ transformed and fitted to the Baranyi and Roberts' model in order to verify the kinetic parameters of microbial growth (maximum specific growth rate and lag phase duration) for the TVC and salmonella (XLD). A detailed description of the preparation of minced beef samples, as well as their related microbiological analysis, is described in [24]. The growth curves of TVC and XLD for minced beef storage at different temperatures under AIR and MAP conditions as a function of storage time are illustrated in Fig. 1.

The growth curves for both TVC cases are similar, with the exception that the maximum specific growth rate (μmax) for the AIR packaged condition is different than of that of the MAP case. It has been found that packaging under modified atmosphere delay the growth rates of all members of the microbial association, as well as the maximum population attained by each microbial group compared with aerobic storage. Aerobic storage accelerates spoilage due to the fast growing *Pseudomonas* spp.; in addition such growth can be significantly inhibited by the presence of gas carbon dioxide [25]. Analysis specified that the total viable counts ranged from 3.8–9.8 $\log_{10}$ cfu cm^{-2} for aerobic cases, and 3.7–8.5 $\log_{10}$ cfu cm^{-2} for MAP cases. However, for both AIR and MAP conditions, the growth rate is increased faster, as the storage temperature increases. For the case of XLD, significant changes occur only when temperature reaches at 15 °C.

2.2 Multispectral imaging acquisition

Images from every sample (56 aerobic and 56 MAP cases) were captured using VideometerLab, (Videometer A/S, Denmark), a system which acquires multispectral images in 18 different wavelengths ranging from 405 to 970 nm.

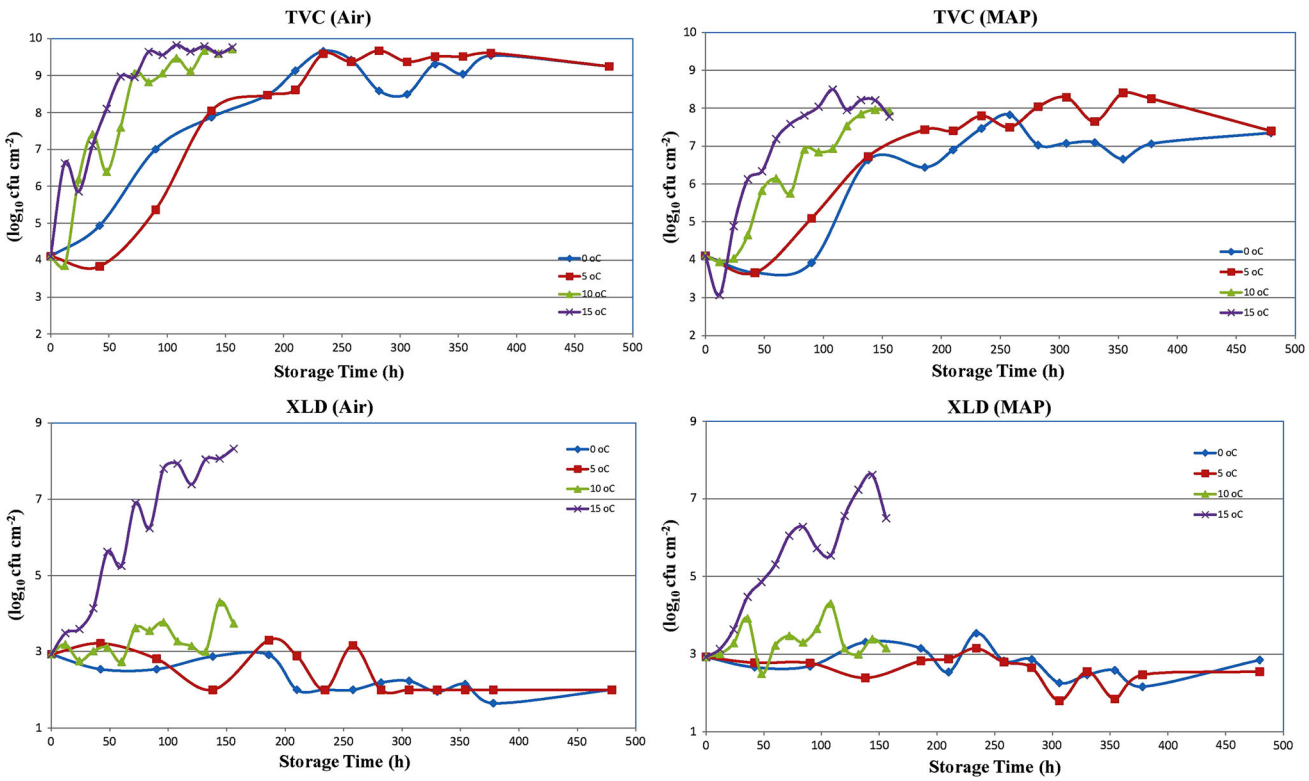

Fig. 1 Population dynamics of TVC and XLD at various temperatures for minced beef samples

More specifically, the wavelengths are at 405, 435, 450, 470, 505, 525, 570, 590, 630, 645, 660, 700, 850, 870, 890, 910, 940 and 970 nm. Meat samples were presented in Petri dishes and collected at the same time as microbiological analysis occurred [26].

The acquisition system records surface reflections with a standard monochrome charge coupled device chip, nested in a calibrated digital camera. The meat sample was placed inside an Ulbricht sphere in which the camera is top-mounted. The sphere has its interior coated with matte titanium paint. The coating together with the curvature of the sphere ensures a uniform reflection of the cast light and thereby a uniform light in the entire sphere. At the rim of the sphere, light emitting diodes (LEDs) with narrow-band spectral radiation distribution are positioned side by side in a pattern, which distributes the LEDs belonging to each wavelength uniformly around the entire rim. These characteristics ensure an optimal dynamic range and keep the amount of shadow and shading effects to a minimum. The result is a monochrome image with 32-bit floating point precision for each LED type, giving in the end, a multispectral 3D cube of dimensionality $1280 \times 960 \times 18$ [27].

As images include redundant information, such as the Petri dish as well as meat fat, a segmentation procedure is required as a pre-processing step. The main objective of segmentation is to identify only the minced meat as the Region of Interest (ROI) from the background or any other undesired regions. This step includes transformation and segmentation procedures, which were implemented using VideometerLab software. The pre-processing was implemented by maximizing the contrast between the sample meat material and the other non-relevant objects, enabling thus a threshold operation [28]. Canonical discriminant analysis (CDA) was employed as a supervised transformation building method to divide the images into regions of interest [29]. Following transformation using CDA, the separation was distinct and a simple thresholding was enough to separate meat from non-meat. The multispectral image sample without the background was transformed to spectrum by mean calculation. For each image, the mean reflectance spectrum was calculated by averaging the intensity of pixels within the ROI at each wavelength. Thus, the resulting data consisted of 18 mean values of the reflectance, as it was recorded by the camera for the pixels that were included in each image's ROI, and were further analyzed with the proposed intelligent decision support system [30]. Figure 2 illustrates samples of mean reflectance spectra acquired for from both AIR and MAP minced beef samples. A close look on selected spectra at Fig. 2 and more precisely on the case of aerobic samples stored at 5 °C reveals that there are some differences in the reflectance's magnitude in the wavelength range from 600 to 850 nm, between unspoiled sample ($t = 0$ h, TVC $= 4.1$ $\log_{10}$ cfu cm^{-2}) and spoiled sample ($t = 479.5$ h, TVC $= 9.3$ $\log_{10}$ cfu cm^{-2}). These differences usually result from the spoilage and deterioration of nutrient compositions such as carbohydrates, protein, fat, which are gradually consumed and decomposed during storage, producing a series of chemical substances, including ammonia, hydrogen sulphide, ketones and aldehydes [9]. A similar situation can be also observed in the near infrared region (850–970 nm) where reflectance values are decreased with increasing storage time [26]. Datasets related to reflectance spectra as well as the associated microbiological analysis from meat samples, were provided by Agricultural University of Athens, Greece and were further utilised towards the development of the proposed intelligent decision support system.

3 AFINN architecture

The proposed neuro-fuzzy (NF) system is a modification of the ANFIS model and incorporates an additional layer of output partitions. Initially, a clustering algorithm has been applied to the training data in order to organize feature vectors into clusters. The fuzzy rule base is then derived using results obtained from the clustering algorithm. The schematic of the AFINN model, shown in Fig. 3, consists of five layers. Layers L_1 and L_2 are associated to IF part of fuzzy rules while layers L_4 and L_5 to THEN part of these rules and are related to the defuzzification task. In layer L_3 a mapping between the rules layer and the output layer is performed through a competitive learning process and as a consequence, the linear units at L_4 are linked with each term of layer L_3. Thus the size of required matrices for least-squares estimation at the consequent part is much smaller compared to the ANFIS approach. The clustering algorithm at layer L_2 consists of two steps [23]. In the first step, a method similar to Learning Vector Quantization (LVQ) algorithm creates crisp c-partitions of the dataset. The number of clusters c and the associated centres $v_i, \quad i = 1, \ldots c$, calculated from this step are utilised by the fuzzy c-means (FCM) algorithm in the second step. The first cluster is created starting with the first data vector from $X = [x_1, \ldots, x_n] \in R^{np}$, which is the learning data set. Cluster centres v_i are then modified for each cluster (i.e. $i = 1, \ldots, c$) according to the following equation

$$v_i(t+1) = v_i(t) + a_t(x_k - v_i(t)) \tag{1}$$

where $t = 0, 1, 2, \ldots$ denotes the number of iterations and $a_t \in [0, 1]$ is the learning rate. These cluster centres which are considered to be the initial values of the fuzzy centres derived by the second step algorithm. In the second step, the FCM algorithm has been used to optimise the values of cluster centres.

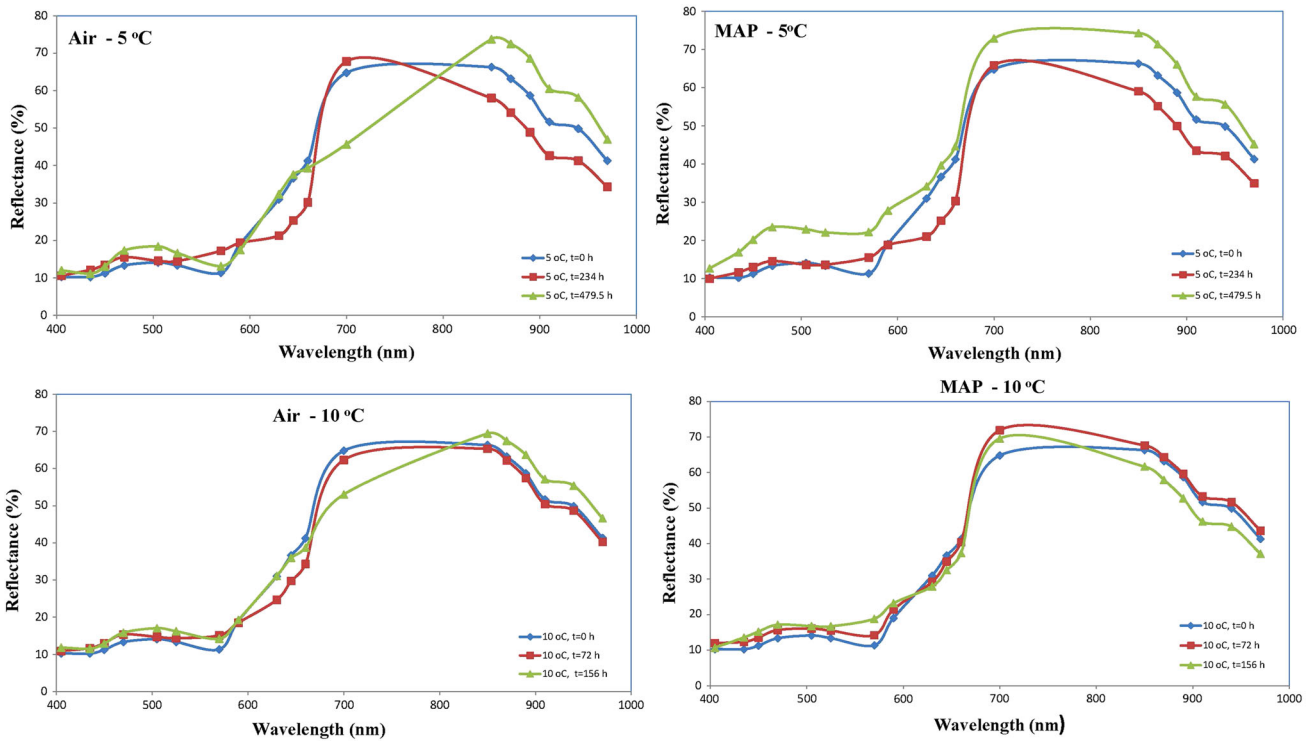

Fig. 2 Selected spectra for both AIR and MAP cases

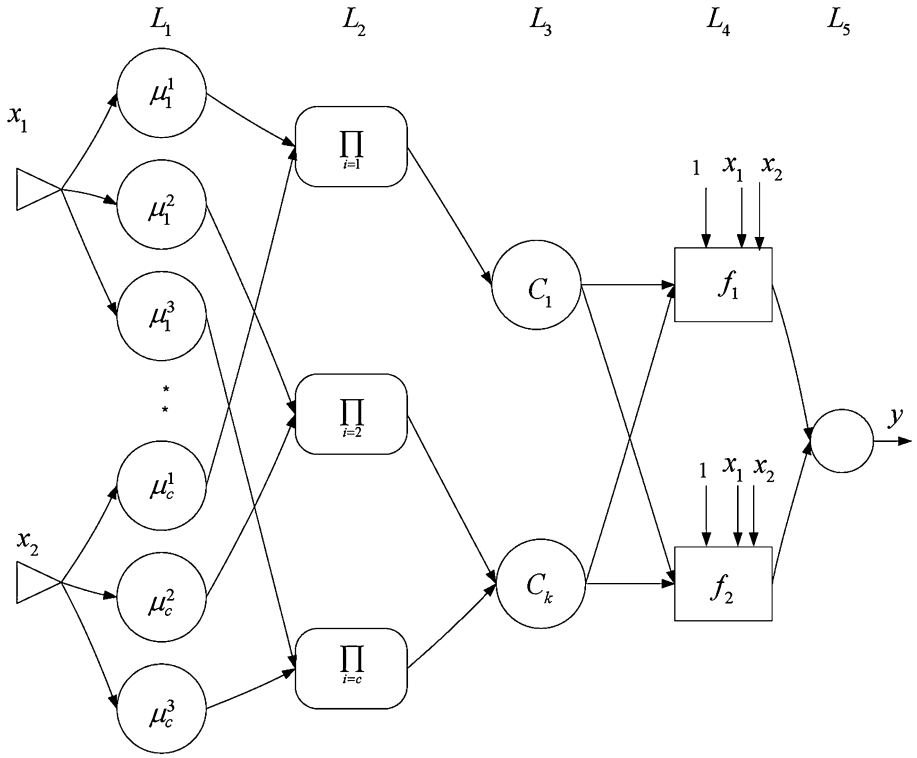

Fig. 3 Structure of AFINN system

3.1 AFINN internal structure

The number of rules in the AFINN scheme is identical to the number of clusters c obtained from the clustering algorithm. Fuzzy IF–THEN rules then can be written in the following form:

$$\begin{aligned} &\text{IF } (x_1 \text{ is } U_1^i \text{ AND}\ldots\text{AND } x_q \text{ is } U_q^i) \\ &\quad \text{THEN } (y = w_0^i + w_1^i x_1 + \cdots + w_q^i x_q) \end{aligned} \tag{2}$$

where $U_j^i, i = 1,\ldots,c; j = 1,\ldots p$ and $q = p - 1$, are fuzzy sets defined based on c-partition of learning data X. The membership functions of fuzzy sets U_j^i have be chosen as Gaussian membership functions with the following form:

$$O_{U_j^i}^1 = \mu_{U_j^i} = \exp\left[-\left(\frac{x_j - v_{ij}}{\sigma_{ij}}\right)^2\right] \tag{3}$$

for $j = 1,\ldots,q$ and $i = 1,\ldots,c$. The values v_{ij} in Eq. (3) represent the centres of the membership functions and are equal to the values of the components of vectors v_i which derive from the FCM algorithm. The values σ_{ij} in Eq. (3) define the widths of the membership functions. These values are calculated according to

$$\sigma_{ij} = \left(\sum_{k=1}^{n} u_{ik}(x_{kj} - v_{ij})^2 \Big/ \sum_{k=1}^{n} u_{ik}\right)^{1/2} \tag{4}$$

The second layer L_2 has c elements that realize a multiplication operation. Outputs of this layer represent the fire strength of the rules, expressed as:

$$O_i^2 = \prod_{j=1}^{q} O_{U_j^i}^1 \tag{5}$$

where $i = 1,\ldots,c$. Nodes at the additional layer (L_3), represent the partitions of the output variables. The nodes should perform the fuzzy OR operation to integrate the fired rules:

$$O_l^3 = \sum_k O_k^2 w_{l,k}^3 \tag{6}$$

where, $k = 1,\ldots,c$. Hence, links between L_2 and L_3 function as an inference engine that does not require the rule-matching process. Initially, the links at layers L_2–L_3 are fully interconnected. However, not all the rules are necessary to the fuzzy system. The weight of the link connecting the kth rule node from L_2 and the lth output partition at L_3 is denoted as $w_{l,k}^3$ and assigned to be 0.5. A competitive learning algorithm is then utilised. For the set of training data pairs (x, y) the weights are adjusted as:

$$\Delta w_{l,k}^3 = O_l^3(-w_{l,k}^3 + O_k^2) \tag{7}$$

where O_l^3 is denoted as the output of the l output term node, while O_k^2 is the output of the k fuzzy rule node. Hence, O_l^3 serves as a win-loss index of competition. As the competitive algorithm needs the number of output nodes O_l^3 to be a priori known, this has been heuristically set to be (1/2 + 1) of the defined number of rules. The main principle of this phase is to remove the less important rules and to retain essential ones based on the results of competitive learning through the whole set of trained data pairs. The weight of a link that connects a rule node and an output partition node indicates the strength of the rule affecting the output partitions. The link with the maximum weight is chosen and it is assigned to 1, while the remaining ones to 0. Therefore, only the rule with the link of maximum weight will be assigned to the output partitions. After that, the weights of the links that connect the same output term node are compared. If the weight of the link is found to be small compared to the maximum one, the weight of the link is assigned to zero. The remaining weights are then assigned to 1. Hence $w_{l,k}^3$ will be either 0 or 1, which indicates the existence of the links connecting the node l in L_3 and the node k in L_2. At layer L_4, every node is an adaptive node, with a node function as:

$$O_l^4 = \frac{O_l^3}{\sum_l O_l^3} f_l = \frac{O_l^3}{\sum_l O_l^3}(p_l x_1 + q_l x_2 + r_l) \tag{8}$$

where $\{p_l, q_l, r_l\}$ is the consequent parameter set of this node. Finally in the last layer, L_5, the single node in this layer computes the overall output as the summation of all incoming signals:

$$O^5 = \sum_l O_l^4 \tag{9}$$

Similarly to the ANFIS model, a hybrid learning approach has been also adopted for the AFINN scheme [23]. All modelling schemes have been implemented in MATLAB (ver. R2014a, Mathworks.com).

4 Decision support system development

An intelligent decision support system, based on the proposed AFINN model, has been designed in such way in order to accommodate all relevant information. The real challenge in this paper is to propose a new learning-based structure which could be considered as a benchmark method towards the development of efficient intelligent methods in food quality analysis. For this reason, AFINN's results are compared with those obtained by MLP neural networks, ANFIS neurofuzzy identification models and PLS regression schemes. Such schemes have been applied recently in the area of food science and technology as

modelling systems [31]. Its overall schematic diagram shown at Fig. 4 includes a classifier unit to discriminate AIR/MAP based samples as well as an identification model to predict the temperatures under which meat samples were stored. Individual identification models have been also developed for the prediction of the total viable counts of bacteria (TVC) as well as the growth of salmonella (XLD) for both AIR/MAP conditions.

Due to the multi-variable nature of multispectral data, a dimensionality reduction algorithm was applied on multispectral data used for training purposes. The robust PCA (RPCA) scheme has been utilized to obtain principal components that are not influenced much by outliers [32].

The RPCA is implemented in three main steps. First, the data are pre-processed such that the transformed data are lying in a subspace whose dimension is at most $n-1$. A preliminary covariance matrix is then constructed and used for selecting the number of components k that will be retained in the sequel, yielding a k-dimensional subspace that fits the data well. Then the data points are projected on this subspace where their location and scatter matrix are robustly estimated, from which its k nonzero eigenvalues $l_1, \ldots, l_k$ are computed. The corresponding eigenvectors are the k robust principal components [32]. RPCA scheme was implemented in MATLAB, with the aid of PLS_Toolbox (ver. 8.0 Eigenvector.com). For this particular experimental case study, the first five principal components (PC) were associated with the 99.675 % of the total variance, as shown in Table 1. These specific PCs were extracted and utilized as input variables to the learning-based models developed for this specific case study.

Table 1 Robust PCA scheme

PCs	Robust PCA		
	Eigenvalue	Prop. %	Cum. prop. %
1	346	65.98	65.98
2	125	22.94	88.92
3	48.8	8.98	97.90
4	8.96	1.56	99.46
5	1.21	0.21	99.67

A mandatory check however is required to validate the integrity and applicability of the developed model in predicting/classifying unknown samples to make sure that models could work in the future for new and similar data. Full cross-validation, also called leave-one-out cross-validation (LOOCV), is commonly utilized to validate the established models [33, 34]. LOOCV leaves one sample out of the calibration process, which is used for validation. All samples are used in an exhaustive way providing thus repeatability of the results compared with other random methods of partitioning of the training dataset. As the number of samples was small, separation of the dataset into training and testing subsets (hold-out method) would further reduce the number of data and would result in insufficient training of the network. Therefore, in order to improve the robustness of classification, the LOOCV method has been adopted to evaluate the performance of the developed models. Meanwhile, it is necessary to look for effective methods to evaluate the predictive effectiveness, robustness, reliability, and accuracy for practical

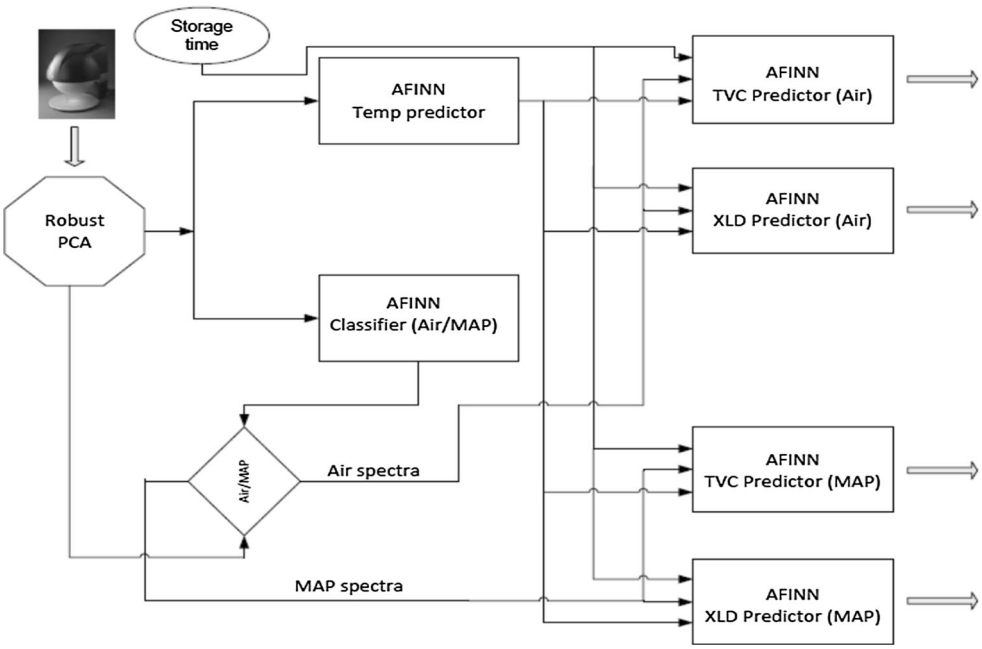

Fig. 4 Structure of proposed decision support system

applications. The performance of developed models for the prediction of TVC and XLD for each meat sample was determined by the bias (B_f) and accuracy (A_f) factors, the mean relative percentage residual (MRPE) and the mean absolute percentage residual (MAPR), the root mean squared error (RMSE) and finally the standard error of prediction (SEP) [34, 35].

5 Results and discussion

The final dataset consisted of 56 minced beef samples at aerobic and 56 samples at MAP conditions respectively. Information related also to sampling times was also considered for this analysis.

5.1 Classification of meat samples

The classification accuracy acquired by the AFINN model for the categorization of storage conditions (Aerobic vs. MAP) is presented in the form of a confusion matrix in Table 2. For this specific model, 22 rules have been created by the clustering scheme, while the input vector consisted of the five PCs extracted from the RPCA algorithm. The hybrid parameter learning algorithm resulted in a high speed training process, i.e. 20 epochs. The sensitivities reveal an overall excellent performance for both cases. The model overall achieved a 95.53 % correct classification, and 96.43 and 94.64 % for AIR and MAP meat samples, respectively. The sensitivities for AIR and MAP-based meat samples reveal 54 (including two marginal cases) AIR samples, and 53 MAP samples properly classified to their own class. Misclassified samples "1A5", "1A10" correspond to minced beef AIR samples stored at 5 and 10 °C respectively and collected immediately (0 h of storage). Similarly, misclassified samples "1M5", "1M10", "1M15" correspond to minced beef MAP samples stored at 5, 10 and 15 °C respectively and collected instantly (0 h of storage). Such misclassification can be explained by the fact, that at $t = 0$, meat samples share the same spectral information.

The specificity index was also high, indicating satisfactory discrimination between these two classes. In addition to AFINN, an ANFIS model has been also developed to classify AIR/MAP samples. Under the same training conditions, ANFIS performed very satisfactory, its performance however was achieved with a relatively computational cost, utilising 32 fuzzy rules, using two membership functions for each input variable. An overall classification accuracy of 93.75 % resulted in 7 misclassifications. In addition to previously misclassified samples, new samples "4A0" and "4M0" were also failed to be identified. These samples correspond to AIR and MAP samples stored at 0 °C, collected after 138 h of storage respectively.

5.2 Temperature identification model

The changes in microbial flora of fresh minced meat has been monitored at different storage temperatures (0–15 °C) under aerobic and MAP conditions. Results from microbiological analysis, revealed that changes in Total Viable Counts follow temperature changes during storage and thus, temperature could be considered as a good indicator for meat spoilage. However, the knowledge of storage temperature is not always available, thus this issue could be considered as an obstacle for production line use.

The motivation for this research study derives from the aim to predict, for the first time, directly the storage temperature by utilising only multispectral information. Such non-invasive temperature "measurement" could be then utilised for the prediction of TVC and XLD levels. The accuracy acquired by an AFINN model for the temperature prediction was 93.75 % and is presented in the form of a confusion matrix in Table 3. Seven minced meat samples were not identified properly. These include the aerobic "1A0", "1A5", "5A10", "1A15" and the MAP "1M0", "1M5", "1M15" samples. The "1A0", "1A5", "1A15" cases correspond to AIR samples stored at 0, 5 and 15 °C

Table 2 Confusion matrix for class of storage conditions

Class (AIR/MAP)	Predicted class (AFINN)		Row total	Sensitivity (%)
	AIR	MAP		
AIR ($n = 56$)	52 (+2 marginal)	2	56	96.43
MAP ($n = 56$)	3	53	56	94.64
Column total (n_j)	57	56	112	
Specificity (%)	94.74	94.64		
Overall correct classification (accuracy): 95.53 %				

Table 3 Confusion matrix for temperature using AFINN model

Temp (AIR/MAP)	Predicted class (AFINN)								Row total	Sensitivity total (%)
	AIR				MAP					
	0 °C	5 °C	10 °C	15 °C	0 °C	5 °C	10 °C	15 °C		
0 °C	13		1		13		1		28	92.85
5 °C		13	1			13	1		28	92.85
10 °C		1	13				14		28	96.43
15 °C			1	13			1	13	28	92.85
Column total (n_j)	13	14	16	13	13	13	17	13	112	
Specificity (%)	100	92.85	81.25	100	100	100	82.35	100		

Overall correct classification (accuracy): (AIR: 92.85 %, MAP: 94.64 %) 93.75 %

Table 4 Confusion matrix for temperature using ANFIS/MLP models

Temp (AIR/MAP)	Predicted class (ANFIS)								Row total	Sensitivity ANFIS (%)	Sensitivity MLP (%)
	AIR				MAP						
	0 °C	5 °C	10 °C	15 °C	0 °C	5 °C	10 °C	15 °C			
0 °C	13		1		13		1		28	92.85	89.28
5 °C		13	1		2	11	1		28	85.71	89.28
10 °C			14				14		28	100	89.28
15 °C			1	13			1	13	28	92.85	92.85
Column total (n_j)	13	13	17	13	15	11	17	13	112		
Specificity (%)	100	100	82.35	100	86.66	100	82.35	100			

Overall correct classification (accuracy)—ANFIS: (AIR: 94.64 %, MAP: 91.07 %) 92.85 %

Overall correct classification (accuracy)—MLP: (AIR: 91.07 %, MAP: 89.28 %) 90.17 %

respectively and collected immediately (0 h of storage). The case "5A10" corresponds to an AIR sample stored at 10 °C and collected at 48 h. Similarly, "1M0", "1M5", "1M15" cases correspond to MAP samples stored at 0, 5 and 15 °C respectively and collected immediately (0 h of storage).

An ANFIS model has been also developed to predict temperature levels. An overall classification accuracy of 92.85 % resulted in 8 misclassifications, as clearly shown in Table 4. In addition to the misclassified samples which were collected immediately (0 h of storage), new samples "9M5" and "13M5" were failed also to be identified. These cases correspond to MAP samples both stored at 5 °C, but collected at 282 h and 378 h respectively. Additionally, an MLP network has been implemented using the same conditions using two hidden layers (with 24 and 12 nodes respectively). Due to the usage of gradient descent learning algorithm, 20,000 epochs were applied, resulting thus a rather slow training procedure. The prediction accuracy obtained from MLP was inferior to those achieved by both AFINN and ANFIS, with an overall rate of 90.17 %.

5.3 Total viable counts identification model

AFINN models have been also constructed for TVC prediction for both Aerobic and MAP cases [36]. For each case, two simulation studies were carried out.

In the first study, AFINN's input vector consisted of the five PCs extracted from the RPCA algorithm, as well as the sampling time and temperature information, while in the second study only the extracted PCs were considered as input variables. The number of rules used in these networks was 34 and 22 for each study respectively.

Results revealed that the identification accuracy of the AFINN model was very satisfactory in the prediction of TVCs for the AIR dataset, indicating the advantage of this approach in tackling nonlinear problems, such as meat spoilage. The plot of predicted versus observed TVCs is illustrated in Fig. 5, and shows a very good distribution around the line of equity, with almost all the data included within the ±0.5 log unit area.

Based on Fig. 5, the "7A5" pattern that corresponds to a minced beef sample stored at 5 °C and collected after

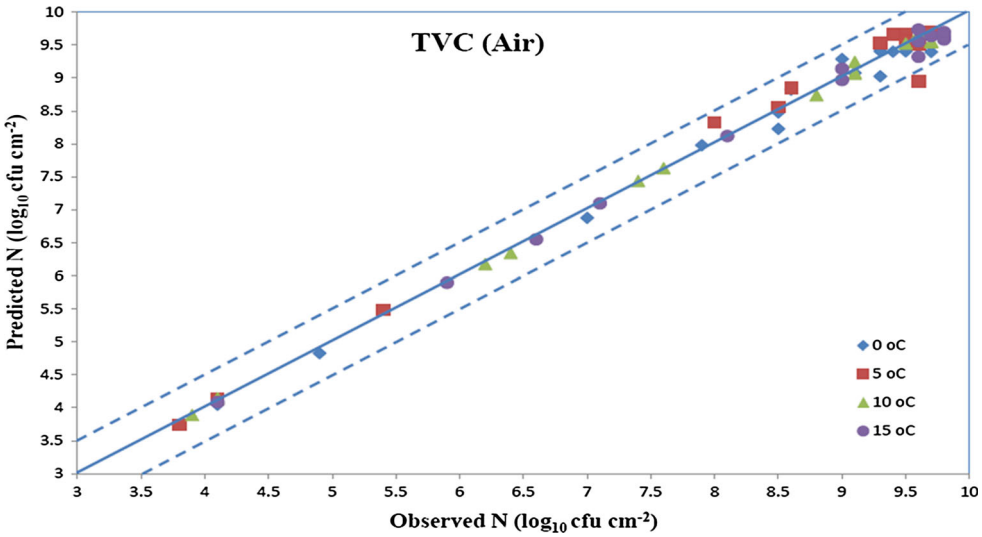

Fig. 5 AFINN prediction model for TVC (AIR case—all inputs)

Table 5 Statistical performance for AIR case (all inputs)

TVC—AIR case (LOOCV) PCA inputs, time, temperature (P, O, denote the predicted and observed values, while n is the number of observations)	Mathematical expression	Temperatures (AFINN)				Total AFINN	Total AFINN (46/10)
		0 °C	5 °C	10 °C	15 °C		
Mean squared error (MSE)	$\frac{1}{n}\sum_{i=1}^{n}(P-O)^2$	0.0304	0.0599	0.0064	0.0153	0.028	0.1335
Root mean squared error (RMSE)	$\sqrt{\frac{\sum(O-P)^2}{n}}$	0.1745	0.2447	0.0797	0.1238	0.1673	0.3654
Mean relative percentage residual (MRPR %)	$\frac{1}{n}\sum\frac{100(O-P)}{O}$	0.5465	−0.787	0.1028	0.5387	0.1003	−1.5921
Mean absolute percentage residual (MAPR %)	$\frac{1}{n}\sum\frac{100\lvert(O-P)\rvert}{O}$	1.6684	2.1346	0.7659	0.9869	1.3889	3.3159
Bias factor (B_f)	$10\sum\log(P/O)/n$	0.9943	1.0075	0.9989	0.9945	0.9988	1.0152
Accuracy factor (A_f)	$10\sum\lvert\log(P/O)\rvert/n$	1.0169	1.0216	1.0077	1.0100	1.014	1.0332
Standard error of prediction (SEP %)	$\frac{100}{O}\sqrt{\frac{\sum(O-P)^2}{n}}$	2.1274	2.9941	1.0124	1.4728	2.0498	4.1566

234 h of storage was placed outside the specified area. The performance of the AFINN model to predict TVCs in minced beef samples in terms of statistical indices is presented in Table 5. The RMSE values of the model were very low for testing samples, with an overall indicator of 0.1673. The accuracy factor A_f, which indicates the spread of results about the prediction, reveal that predicted total viable counts were 1.4 % above from the observed values for meat samples. The mean relative percentage residual index (MRPR) verified the overall under-prediction for samples (MRPR > 0). Finally, the standard error of prediction (SEP) index was 2.049 % for the overall samples indicating a good performance of the network for microbial count predictions.

In order to investigate further the capabilities of AFINN model for this specific identification problem, a second experiment was carried out, where the initial multi-AIR dataset was divided into a training subset with approx. 82 % of the data and a testing subset with the remaining 18 % (i.e. 10 samples). The performance of the AFINN model to predict TVCs in minced beef samples for this second experiment, in terms of statistical indices is also presented in Table 5. Based on the new calculated values of the bias factor B_f, it can be assumed that model has overestimated ($B_f > 1$) microbial population. However, a closer comparison of AFINN's performance at these two experiments reveals a problem with the limited number of samples for training. The SEP index is worse in this second case, and this reflects an open problem in learning-based systems, i.e. the need to have as large as possible training datasets.

An ANFIS and MLP models have been developed to predict TVCs utilising the same training conditions. ANFIS model performed very satisfactory, as shown in Table 6, its performance however was achieved with a high computational cost, utilising 128 fuzzy rules and subsequently a

Table 6 Statistical performance for AIR case (all inputs-comparison)

TVC—AIR case (LOOCV) PCA inputs, time, temperature	Total ANFIS	Total MLP	Total NLR	Total PLS
Mean squared error (MSE)	0.0579	0.0744	0.0909	0.9022
Root mean squared error (RMSE)	0.2406	0.2727	0.3015	0.9498
Mean relative percentage residual (MRPR %)	−0.2408	−0.486	−0.2166	−2.396
Mean absolute percentage residual (MAPR %)	2.4768	3.0725	3.3923	11.263
Bias factor (B_f)	1.0019	1.0041	1.0010	1.0109
Accuracy factor (A_f)	1.0250	1.0310	1.0342	1.1105
Standard error of prediction (SEP %)	2.9479	3.3412	3.6938	11.6366

large number of consequent parameters. After a few trials, the MLP was constructed with two hidden layers (with 12 and 10 nodes respectively) and one output node for the TVC prediction.

The performance of the MLP network in predicting TVC in meat samples in terms of statistical indices is also presented in Table 6. Although both AFINN and ANFIS share the same TSK-style architecture, the clustering component allowed AFINN to achieve a superior performance. On the other hand, the localisation spread through the membership functions, is one advantage of ANFIS and AFINN models against the classic MLP structure.

In addition to these computational intelligence structures, partial least squares (PLS) and nonlinear regression schemes have been applied to the same dataset, in order reveal the advantage of advanced learning-based methods. The PLS model was constructed using the same input vector as in the cases of AFINN, and the PLS_Toolbox software (ver. 8.0, Eigenvector.com) in association with MATLAB was used to perform the PLS analysis. The SIMPLS algorithm has been chosen as the appropriate optimisation scheme [37]. The algorithm calculates the PLS factors directly as linear combinations of the original variables. These factors are determined such as to maximize a covariance criterion, while obeying certain orthogonality and normalization restrictions. The optimal number for latent variables was set to 7. The following PLS model is associated with this specific case study.

$$\begin{aligned} Y1 = {} & 6.63310 + 0.00555 \times X1 + 0.07886 \times X2 \\ & - 0.00677 \times X3 + 0.05901 \times X4 + 0.14028 \times X5 \\ & + 0.06439 \times X6 + 0.11419 \times X7 \end{aligned} \quad (10)$$

where X_1 represents the sampling time, X_2 the temperature, and the remaining X_i inputs the five PCs from the RPCA scheme. Nonlinear regression is often used to model complex phenomena which cannot be handled by the linear model. The XLSTAT (v. 2015.2) software provides such capability through the use of nonlinear regression (NLR) modelling using the nonlinear iterative partial least squares (NIPALS) algorithm. For this specific case, the following 4th order model has been constructed using XLSTAT and achieved a remarkable performance compared to PLS scheme. Its performance could be easily compared to MLP's results.

$$\begin{aligned} Y1 = {} & 4.96194 + 0.05334 \times X1 - 0.33833 \times X2 \\ & - 0.00504 \times X3 + 0.00893 \times X4 \\ & + 0.11732 \times X5 + 0.00651 \times X6 \\ & - 0.11490 \times X7 - 0.00026 \times X1^2 \\ & + 0.07909 \times X2^2 - 0.00127 \times X3^2 \\ & + 0.00079 \times X4^2 - 0.01233 \times X5^2 \\ & - 0.02901 \times X6^2 + 0.27772 \times X7^2 \\ & + 6.03629\text{E}{-7} \times X1^3 - 0.00344 \times X2^3 \\ & - 5.67724\text{E}{-6} \times X3^3 + 0.00001 \times X4^3 \\ & - 0.00074 \times X5^3 + 0.00156 \times X6^3 \\ & + 0.03664 \times X7^3 - 5.13162\text{E}{-10} \times X1^4 \\ & + 7.81010\text{E}{-7} \times X3^4 - 1.47147\text{E}{-6} \times X4^4 \\ & + 0.00006 \times X5^4 + 0.00025 \times X6^4 \\ & - 0.04060 \times X7^4 \end{aligned} \quad (11)$$

Statistical information for both NLR and PLS models is illustrated at Table 6. However, such performance from PLS scheme was expected, as it is well known that linear PLS has some difficulties in its practical applications since most real problems are inherently nonlinear.

For the second simulation study, the input vector was consisted of the five only PCs extracted from the RPCA algorithm. The plot of predicted versus observed TVCs is illustrated in Fig. 6, and shows a good distribution around the line of equity. The comparison of Fig. 5 with the related Fig. 6 is more than evident. One sample, the "2A15", is clearly outside the border line of the ±0.5 log unit area and it is associated to a meat sample stored at 15 °C and collected after 12 h of storage. Three samples (i.e. "2A10", "2A5", "4A10") are however in the border

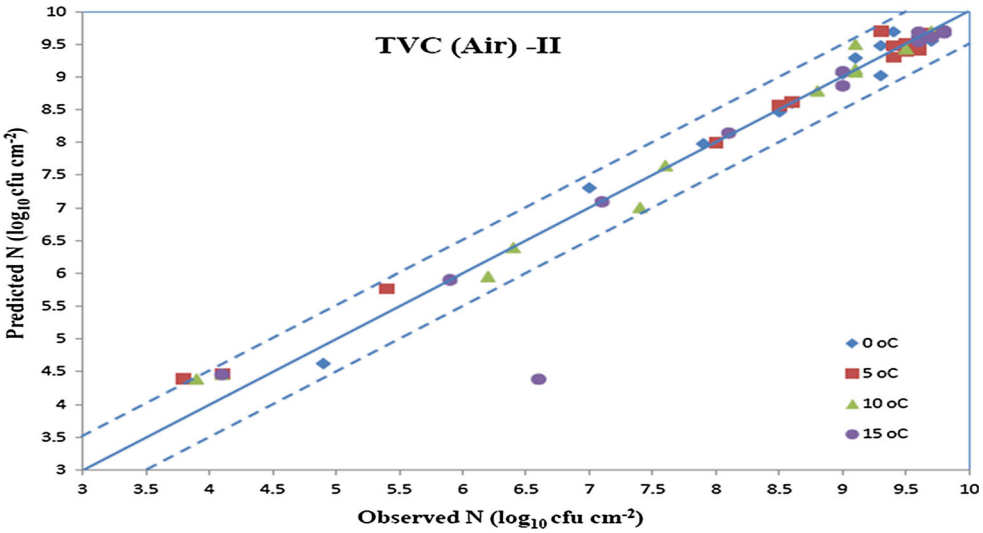

Fig. 6 AFINN prediction model for TVC (AIR case—RPCA inputs)

Table 7 Statistical performance for AIR case (PCA inputs)

TVC—AIR case (LOOCV) PCA inputs	Temperatures (AFINN)				Total AFINN	Total ANFIS	Total MLP	Total NLR	Total PLS
	0 °C	5 °C	10 °C	15 °C					
Mean squared error (MSE)	0.0399	0.0607	0.0535	0.3661	0.1301	0.1989	0.2564	0.3004	1.1807
Root mean squared error (RMSE)	0.1998	0.2463	0.2314	0.6051	0.3606	0.446	0.5063	0.5481	1.0866
Mean relative percentage residual (MRPR %)	−0.755	−2.208	−1.139	2.0953	−0.5018	−0.6087	−0.1852	−0.7906	−3.0959
Mean absolute percentage residual (MAPR %)	2.3601	3.0684	2.7021	3.6667	2.9493	4.3986	5.2674	5.5568	12.8970
Bias factor (B_f)	1.0070	1.0210	1.0104	0.9739	1.0029	1.0032	0.998	1.0046	1.0127
Accuracy factor (A_f)	1.0237	1.0299	1.0267	1.0426	1.0307	1.0455	1.0548	1.0567	1.1245
Standard error of prediction (SEP %)	2.4369	3.0141	2.9399	7.1969	4.4182	5.4645	6.2031	6.7148	13.3119

line of the ±0.5 log unit area. "2A5" corresponds to a minced beef, stored at 5 °C and collected after 42 h of storage, while "2A10" and "4A10" were stored at 10 °C and collected after 12 h and 36 h of storage respectively. The performance of the AFINN model to predict TVCs in minced beef samples for this second simulation, in terms of statistical indices is presented in Table 7. Based on the calculated values, undoubtedly the SEP index is worse in this second scenario, and this is mainly explained by the absence of the sampling time of meat samples from the input vector. There is an open problem of incorporating the time into the spectral information, which could be investigated in a future research. AFINN's performance is still however superior to other applied models, especially against PLS which is considered as a standard modelling tool in food microbiology.

An important advancement in food packaging techniques is the development of Modified Atmosphere Packaging (MAP). Modified atmospheric packaged foods have become increasingly more available, as food manufactures are interested for foods with extended shelf life. In addition to aerobic TVCs prediction, AFINN models have been also applied for minced beef samples packaged under modified atmosphere conditions. The plot of predicted versus observed TVCs for MAP spectra is illustrated in Fig. 7, and shows a good distribution around the line of equity, with almost all the data included within the ±0.5 log unit area, only for the case where additional features (i.e. sampling time, temperature) were included as input variables. Based on Fig. 7, "2M15" and "14M5" patterns were clearly outside the borderline. "2M15" corresponds to a minced beef sample stored at 15 °C and collected after 12 h of storage, while "14M5" corresponds to a sample stored at 5 °C and collected after 479.5 h of storage. Three samples (i.e. "10M15", "12M5", "7M0") were however in the border line of the ±0.5 log unit area. "10M15" corresponds to a minced beef, stored at 15 °C and collected after 108 h of storage, while "12M5" was stored at 5 °C and collected after 354 h. Finally, meat sample "7M0" corresponds to a minced beef, stored at 0 °C and collected after

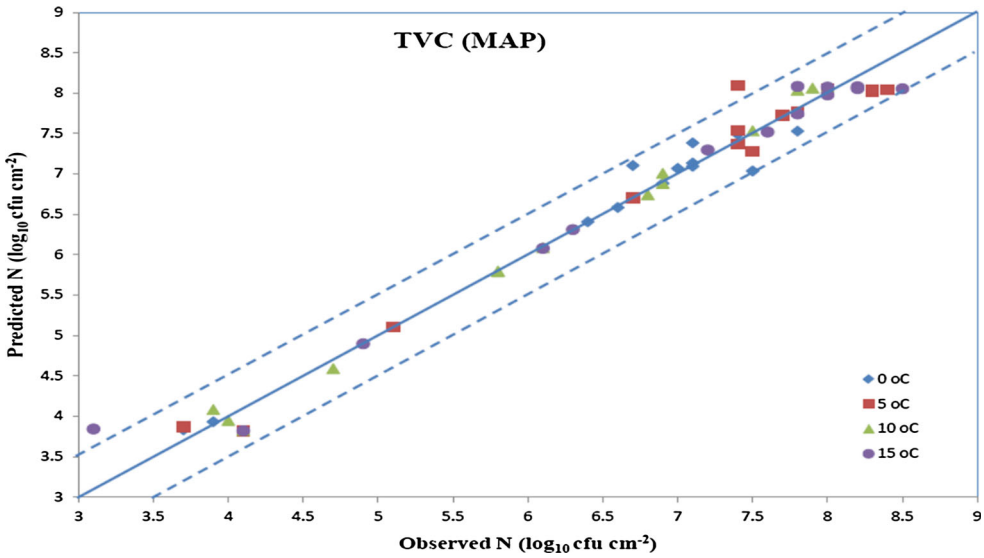

Fig. 7 AFINN prediction model for TVC (MAP case—all inputs)

Table 8 Statistical performance for MAP case (all inputs)

Statistical index—MAP case (LOOCV) PCA inputs, time, temperature	Temperatures (AFINN)				Total AFINN	Total AFINN (46/10)
	0 °C	5 °C	10 °C	15 °C		
Mean squared error (MSE)	0.046	0.0668	0.0163	0.0693	0.0496	0.0960
Root mean squared error (RMSE)	0.214	0.2585	0.1276	0.2632	0.2227	0.3098
Mean relative percentage residual (MRPR %)	−0.021	0.2853	−0.057	−0.890	−0.1708	1.7648
Mean absolute percentage residual (MAPR %)	2.446	2.7323	1.7543	3.4124	2.5863	3.5787
Bias factor (B_f)	0.999	0.9964	1.0002	1.0068	1.0008	0.9779
Accuracy factor (A_f)	1.025	1.0277	1.0178	1.0331	1.0258	1.0372
Standard error of prediction (SEP %)	3.362	3.7002	2.0716	3.8460	3.3784	4.2436

234 h of storage. The performance of the AFINN model to predict TVCs in minced beef samples for the MAP case, in terms of statistical indices is presented in Table 8. The RMSE values of the AFINN model were very low, with an overall indicator of 0.22. A SEP value of 3.38 % was calculated for this specific study, which is however higher compared to the equivalent achieved SEP index for the AIR samples.

Overall, a comparison against AFINN's performance for AIR case, reveal an increased level of difficulty in predicting TVCs for samples packaged in MAP conditions. Similarly to the AIR case, an experiment was carried out, where the initial multi-MAP dataset was divided into a training subset with approx. 82 % of the data and a testing subset with the remaining 18 % (i.e. 10 samples). The performance of the AFINN model to predict TVCs for this experiment, in terms of statistical indices is also presented in Table 8. Based on the new calculated values of the bias factor B_f, it can be assumed that model has under-estimated ($B_f < 1$) microbial population, while the SEP index was increased to 4.24 %. Furthermore, an ANFIS and MLP model have been developed to predict TVCs for the MAP case.

Similarly to the previous aerobic case study, both ANFIS and MLP performed very satisfactory, as shown in Table 9, MLP's performance however was achieved with a computational cost, by utilising two hidden layers (with 18 and 12 nodes respectively), while ANFIS model utilised 128 fuzzy rules. In addition to these learning-based structures, PLS and NLR schemes have been also applied to the same dataset. The following PLS regression model is associated with this MAP dataset

$$\begin{aligned} Y1 = {} & 5.01285 + 0.00516 \times X1 + 0.08757 \times X2 \\ & + 0.01390 \times X3 + 0.07088 \times X4 \\ & - 0.03170 \times X5 + 0.01656 \times X6 \\ & + 0.00409 \times X7 \end{aligned} \quad (12)$$

For this specific case, the following 5th order NLR model has been also constructed using XLSTAT 2015 and the results are also summarised at Table 9.

Table 9 Statistical performance for MAP case (all inputs-comparison)

Statistical index—MAP case (LOOCV) PCA inputs, time, temperature	Total ANFIS	Total MLP	Total NLR	Total PLS
Mean squared error (MSE)	0.0707	0.1103	0.181	1.0268
Root mean squared error (RMSE)	0.266	0.3321	0.4254	1.0133
Mean relative percentage residual (MRPR %)	−0.2573	−0.3622	−0.6577	−3.5658
Mean absolute percentage residual (MAPR %)	3.4666	4.2612	5.5206	15.3059
Bias factor (B_f)	1.0012	1.0015	1.0027	1.0172
Accuracy factor (A_f)	1.0349	1.0428	1.0559	1.1548
Standard error of prediction (SEP %)	4.0351	5.038	6.4542	15.3741

$$
\begin{aligned}
Y1 = {} & 2.69484 + 0.02708 \times X1 - 0.03163 \times X2 \\
& - 0.03285 \times X3 + 0.09362 \times X4 \\
& - 0.02093 \times X5 + 0.10341 \times X6 \\
& + 0.27366 \times X7 + 0.00010 \times X1^2 + 0.02910 \times X2^2 \\
& + 0.00084 \times X3^2 - 0.00448 \times X4^2 + 0.01279 \times X5^2 \\
& - 0.00246 \times X6^2 - 0.24896 \times X7^2 - 1.14461\text{E}{-6} \times X1^3 \\
& - 0.00138 \times X2^3 + 0.00008 \times X3^3 - 0.00050 \times X4^3 \\
& + 0.00020 \times X5^3 - 0.00723 \times X6^3 - 0.12594 \times X7^3 \\
& + 2.94030\text{E}{-9} \times X1^4 - 4.93287\text{E}{-7} \times X3^4 \\
& + 0.00005 \times X4^4 - 0.00009 \times X5^4 \\
& - 0.00006 \times X6^4 + 0.04442 \times X7^4 \\
& - 3.61721\text{E}{-8} \times X3^5 - 1.43622\text{E}{-6} \times X4^5 \\
& - 2.69827\text{E}{-6} \times X5^5 \qquad (13)
\end{aligned}
$$

AFINN model was also tested with the reduced input vector for this MAP study. The plot of predicted versus observed TVCs is illustrated in Fig. 8, and shows a distribution around the line of equity, with eleven samples placed however outside the ±0.5 log unit area. This specific plot, compared with the equivalent for aerobic case, reveals the difficulty in predicting correctly meat samples under MAP conditions. Five patterns (i.e. "2M15", "4M15", "5M15", "7M15", "11M15") were associated to meat samples stored at 15 °C and collected after 12 h, 36 h, 48 h, 72 h and 120 h respectively. Three patterns (i.e. "4M5", "9M5", "13M5") were associated to meat samples stored at 5 °C and collected after 138 h, 282 h and 378 h respectively. Two patterns (i.e. "4M0", "8M0") were associated to meat samples stored at 0 °C and collected after 138 h and 258 h respectively. Finally, one pattern, "4M10", was associated to meat samples stored at 10 °C and collected after 36 h of storage.

The performance of AFINN model to predict TVCs in minced beef samples for this MAP case study, in terms of statistical indices is presented in Table 10. The sole use of PCs in the input vector resulted in a severe deterioration of the prediction accuracy, as clearly shown by all statistical indices. Table 10, however, reveals an additional important issue. Both neurofuzzy schemes (i.e. AFINN and ANFIS)

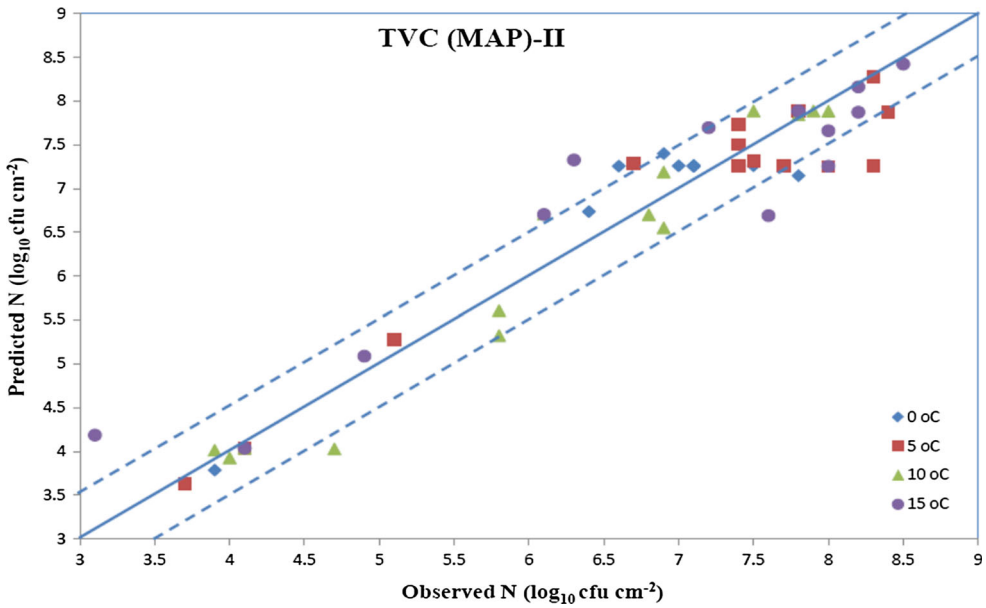

Fig. 8 AFINN prediction model for TVC (MAP case—RPCA inputs)

Table 10 Statistical performance for MAP case (PCA inputs)

TVC MAP case (LOOCV)—PCA inputs	Temperatures (AFINN case)				Total AFINN	Total ANFIS	Total MLP	Total NLR	Total PLS
	0 °C	5 °C	10 °C	15 °C					
Mean squared error (MSE)	0.1287	0.1919	0.1062	0.3223	0.1873	0.3374	0.5844	0.7543	1.4963
Root mean squared error (RMSE)	0.3587	0.4380	0.3260	0.5677	0.4327	0.5808	0.7644	0.8685	1.2232
Mean relative percentage residual (MRPR %)	0.0436	1.5998	1.0274	−2.998	−0.4913	−1.2785	−2.8391	−2.6597	−4.9347
Mean absolute percentage residual (MAPR %)	4.3587	4.3702	4.2935	7.6113	5.1584	7.0959	10.5108	11.9987	18.8424
Bias factor (B_f)	1.0147	0.9825	0.9880	1.0243	1.0022	1.0058	1.0183	1.0131	1.0234
Accuracy factor (A_f)	1.0439	1.0456	1.0446	1.0748	1.0522	1.0692	1.1088	1.1211	1.1912
Standard error of prediction (SEP %)	5.6239	6.2704	5.2939	8.2961	6.5656	8.8126	11.5981	13.1766	18.5589

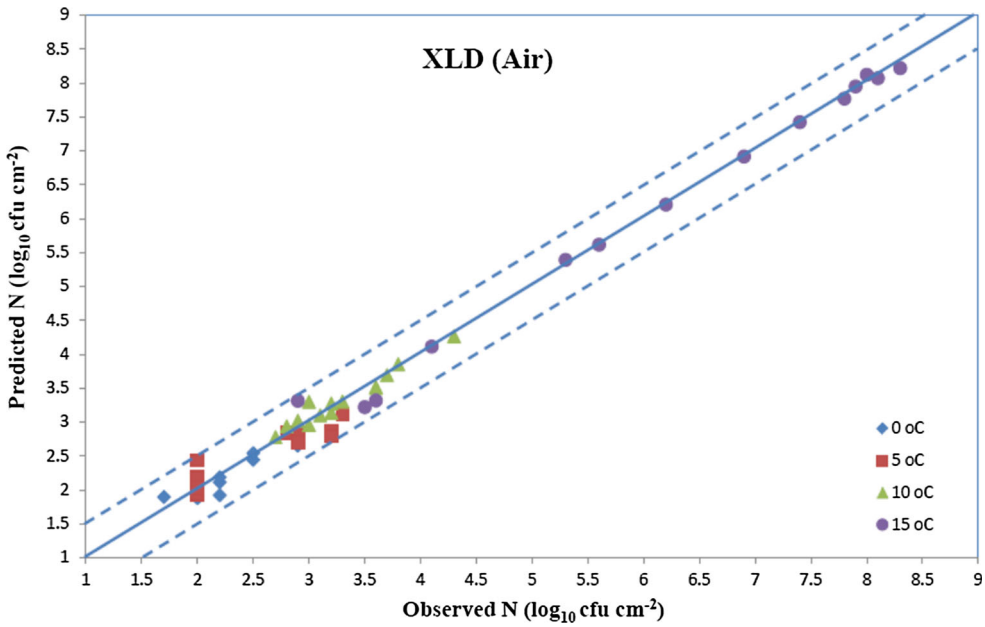

Fig. 9 AFINN prediction model for XLD (AIR case—all inputs)

managed to keep their SEP index below to 10 %, while in the same time, the MLP neural network achieved a not satisfactory prediction performance. In fact, MLP's performance could be comparable to the one achieved by the NLR scheme which has been also applied to the same dataset.

5.4 Salmonella identification model

Finally, two AFINN models have been developed for the prediction of growth levels of Salmonella (XLD) for both AIR and MAP conditions. The number of rules created by the clustering unit in these two AFINN networks was 28 and 32 for AIR and MAP cases respectively.

Results revealed that the accuracy of the AFINN model was very satisfactory in the prediction of XLD for the AIR dataset. The plot of predicted versus observed XLD is illustrated in Fig. 9, and shows a very good distribution around the line of equity, with all the data included within the ±0.5 log unit area. Based on Fig. 9, an excellent fitting has been achieved for the minced samples stored at 15 °C and 10 °C. This can be also verified through the statistical indices which are presented in Table 11.

Based on the calculated values, the SEP index is very low for these temperatures, while the overall SEP value is considered as acceptable for this specific problem, taking into account the XLD growth graphs at Fig. 1. Furthermore, ANFIS and MLP models have been developed to predict XLD for the aerobic case. Similarly to the previous aerobic case studies, both ANFIS and MLP performed very satisfactory, as shown in Table 11.

The prediction of salmonella growth levels under MAP conditions, proved to be less accurate from the equivalent AIR case, similarly to the previous TVC predictions. The

Table 11 Statistical performance for AIR case (XLD case)

XLD—Statistical index AIR case (LOOCV) PCA inputs, time, temperature	Temperatures (AFINN)				Total AFINN	Total ANFIS	Total MLP
	0 °C	5 °C	10 °C	15 °C			
Mean squared error (MSE)	0.0162	0.0476	0.0116	0.0260	0.025	0.0430	0.0644
Root mean squared error (RMSE)	0.1273	0.2183	0.1076	0.1612	0.159	0.2072	0.2539
Mean relative percentage residual (MRPR %)	2.4355	−1.029	−1.1968	−0.1493	0.015	−0.1971	−0.7459
Mean absolute percentage residual (MAPR %)	4.4350	7.2118	2.5285	2.6404	4.204	5.6081	5.8530
Bias factor (B_f)	0.9742	1.0064	1.0114	1.0003	0.998	0.9992	1.0030
Accuracy factor (A_f)	1.0462	1.0736	1.0251	1.0265	1.043	1.0577	1.0607
Standard error of prediction (SEP %)	5.5684	8.9097	3.2613	2.6359	4.501	5.8586	7.1760

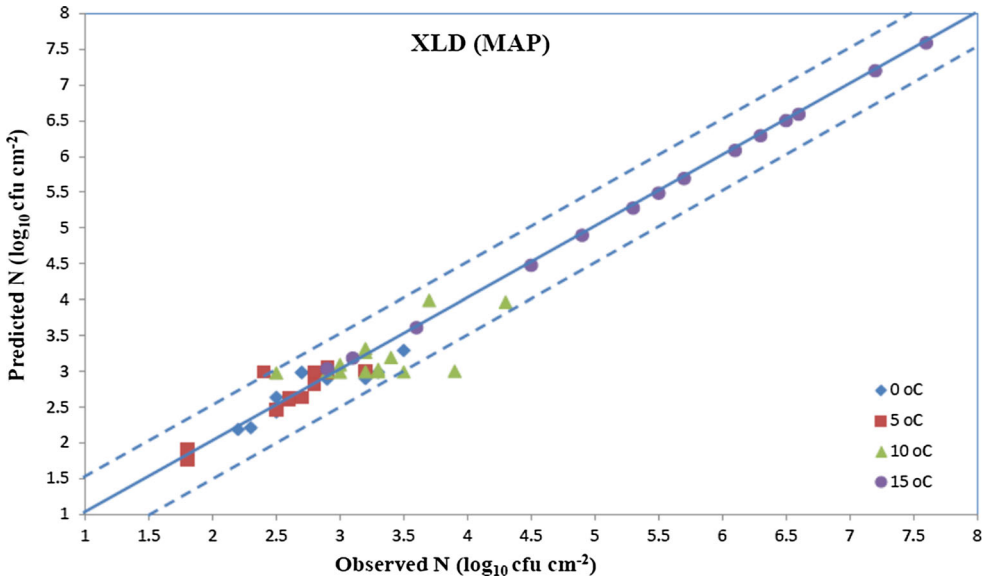

Fig. 10 AFINN prediction model for XLD (MAP case—all inputs)

Table 12 Statistical performance for MAP case (XLD case)

XLD—Statistical index MAP case (LOOCV) PCA inputs, time, temperature	Temperatures (AFINN)				Total AFINN	Total ANFIS	Total MLP
	0 °C	5 °C	10 °C	15 °C			
Mean squared error (MSE)	0.0327	0.0367	0.1267	0.0020	0.0495	0.0661	0.1054
Root mean squared error (RMSE)	0.1808	0.1917	0.3560	0.0449	0.2226	0.2571	0.3247
Mean relative percentage residual (MRPR %)	−0.477	−3.272	2.5640	−0.430	−0.4041	−1.076	−0.2048
Mean absolute percentage residual (MAPR %)	4.9747	4.8535	8.2098	0.7047	4.6857	6.0833	7.9474
Bias factor (B_f)	1.0029	1.0305	0.9692	1.0042	1.0015	1.0071	0.9948
Accuracy factor (A_f)	1.0509	1.0473	1.0884	1.0070	1.048	1.0624	1.0814
Standard error of prediction (SEP %)	6.4911	7.3320	10.741	0.8298	6.3018	7.2788	9.1919

plot of predicted versus observed XLD is illustrated in Fig. 10 and shows a good distribution around the line of equity, with all the data, except one, included within the ±0.5 log unit area. Based on Fig. 10, an excellent fitting has been achieved for the minced samples stored at 15 °C.

The performance of the AFINN model to predict XLD in minced beef samples for this MAP case study, in terms of statistical indices is presented in Table 12. ANFIS model performed very satisfactory, achieving a comparable to AFINN's SEP prediction.

6 Conclusions

In conclusion, this simulation study demonstrated the effectiveness of the detection approach based on multispectral imaging which in combination with a learning-based identification model could be considered as an alternative technique for monitoring meat spoilage. Although MLP and PLS schemes have already been applied to similar multispectral/hyperspectral studies, the exploitation of neurofuzzy models for this specific imaging related application is completely novel and this is the main contribution of this paper. The realization of AFINN model follows the classic TSK structure, incorporating however a clustering unit in the fuzzification section and an additional internal competitive clustering layer. Overall prediction for TVC and XLD cases has been considered as very satisfactory, although lower performance was observed especially for the MAP cases. ANFIS's prediction performance appeared to be comparable to AFINN's case; however such results were achieved with huge expensive computational cost. Prediction performances of MLP, and PLS schemes revealed the deficiencies of these systems which have been used extensively in the area of Food Microbiology. The problem of small amount of real experimental dataset has been tackled in this paper through the LOOCV approach. Research work is in progress to generate "virtual" data from limited experimental spectral samples based on a modified version of the mega-trend-diffusion technique [38]. Future work will be also focused on incorporating in the decision support system information from additional sensors, such as FTIR.

Acknowledgments The second author would like to thank Dr E.Z. Panagou from Agricultural University of Athens, Greece for providing the multispectral dataset, as well as the related microbiological analysis that correspond to minced beef samples.

References

1. Kamruzzaman M, Makino Y, Oshita S (2015) Hyperspectral imaging in tandem with multivariate analysis and image processing for non-invasive detection and visualization of pork adulteration in minced beef. Anal Methods 7(18):7496–7502
2. Amamcharla JK, Panigrahi S, Logue CM, Marchello M, Sherwood JS (2010) Fourier transform infrared spectroscopy (FTIR) as a tool for discriminating *Salmonella typhimurium* contaminated beef. Sens Instrum Food Qual Saf 4(1):1–12
3. Meisel S, Stöckel S, Rösch P, Popp J (2014) Identification of meat-associated pathogens via Raman microspectroscopy. Food Microbiol 38:36–43
4. Balasubramanian S, Panigrahi S, Logue CM, Gu H, Marchello M (2009) Neural networks integrated metal oxide based artificial olfactory system for meat spoilage identification. J Food Eng 91:91–98
5. Tan JL (2004) Meat quality evaluation by computer vision. J Food Eng 61:27–35
6. Faucitano L, Huff P, Teuscher F, Gariepy C, Wegner J (2005) Application of computer image analysis to measure pork marbling characteristics. Meat Sci 69:537–543
7. Peng Y, Lu R (2006) Improving apple fruit firmness predictions by effective correction of multispectral scattering images. Postharvest Biol Technol 41:266–274
8. Lunadei L, Diezma B, Lleo L, Ruiz-Garcia L, Cantalapiedra S, Ruiz-Altisent M (2012) Monitoring of fresh-cut spinach leaves through a multispectral vision system. Postharvest Biol Technol 63:74–84
9. Ma F, Yao J, Xie T, Liu C, Chen W, Chen C, Zheng L (2014) Multispectral imaging for rapid and non-destructive determination of aerobic plate count (APC) in cooked pork sausages. Food Res Int 62:902–908
10. Dissing B, Papadopoulou O, Tassou C, Ersbøll B, Carstensen J, Panagou E, Nychas G-J (2013) Using multispectral imaging for spoilage detection of pork meat. Food Bioprocess Technol 6(9):2268–2279
11. Tao F, Peng Y (2014) A method for non-destructive prediction of pork meat quality and safety attributes by hyperspectral imaging technique. J Food Eng 126:98–106
12. Sun X, Chen KJ, Maddock-Carlin KR, Anderson VL, Lepper AN, Schwartz CA, Keller WL, Ilse BR, Magolski JD, Berg EP (2012) Predicting beef tenderness using color and multispectral image texture features. Meat Sci 92(4):386–393
13. Kamruzzaman M, Sun D-W, ElMasry G, Allen P (2013) Fast detection and visualization of minced lamb meat adulteration using NIR hyperspectral imaging and multivariate image analysis. Talanta 103(15):130–136
14. Kamruzzaman M, Makino Y, Oshita S (2016) Rapid and non-destructive detection of chicken adulteration in minced beef using visible near-infrared hyperspectral imaging and machine learning. J Food Eng 170:8–15
15. Liu D, Pu H, Sun D-W, Wang L, Zeng X-A (2014) Combination of spectra and texture data of hyperspectral imaging for prediction of pH in salted meat. Food Chem 160:330–337
16. Feng Y-Z, Sun D-W (2012) Application of hyperspectral imaging in food safety inspection and control: a review. Crit Rev Food Sci Nutr 52:1039–1058
17. Qin J, Chao K, Kim MS, Lu R, Burks TF (2013) Hyperspectral and multispectral imaging for evaluating food safety and quality. J Food Eng 118:157–171
18. Chen Q, Zhang Y, Zhao J, Hui Z (2013) Nondestructive measurement of total volatile basic nitrogen (TVB-N) content in salted pork in jelly using a hyperspectral imaging technique combined with efficient hypercube processing algorithms. Anal Methods 5:6382–6388
19. Qiao J, Wang N, Ngadi MO, Gunenc A, Monroy M, Gariépy C, Prasher SO (2007) Prediction of drip-loss, pH, and color for pork using a hyperspectral imaging technique. Meat Sci 76(1):1–8
20. Panagou EZ, Kodogiannis V (2009) Application of neural networks as a non-linear modelling technique in food mycology. Expert Syst Appl 36:121–131
21. Ham FM, Kostanic I (2001) Principles of neurocomputing for science and engineering. Arnold Publishers, London
22. Rutkowska D (2002) Neuro-fuzzy architectures and hybrid learning. Springer, Berlin
23. Kodogiannis VS, Petrounias I (2012) Modelling of survival curves in food microbiology using adaptive fuzzy inference neural networks. In: 2012 IEEE international conference on computational intelligence for measurement systems and applications (CIMSA 2012), pp 35–40
24. Ammor MS, Argyri A, Nychas G-J (2009) Rapid monitoring of the spoilage of minced beef stored under conventionally and active packaging conditions using Fourier transform infrared

spectroscopy in tandem with chemometrics. Meat Sci 81(3):507–514
25. Skandamis P, Nychas GJ (2002) Preservation of fresh meat with active and modified atmosphere packaging conditions. Int J Food Microbiol 79:35–45
26. Panagou EZ, Papadopoulou O, Carstensen JM, Nychas G-JE (2014) Potential of multispectral imaging technology for rapid and non-destructive determination of the microbiological quality of beef filets during aerobic storage. Int J Food Microbiol 174:1–11
27. Dissing BS, Nielsen ME, Ersbøll BK, Frosch S (2011) Multispectral imaging for determination of astaxanthin concentration in salmonids. PLoS ONE 6(5):19032
28. Daugaard SB, Adler-Nissen J, Carstensen JM (2010) New vision technology for multidimensional quality monitoring of continuous frying of meat. Food Control 21:626–632
29. Cruz-Castillo JG, Ganeshanandam S, Mackay BR, Lawes GS, Lawoko CRO, Woolley DJ (1994) Applications of canonical discriminant analysis in horticultural research. HortScience 29(10):1115–1119
30. Ropodi AI, Pavlidis DE, Mohareb F, Panagou EZ, Nychas G-JE (2015) Multispectral image analysis approach to detect adulteration of beef and pork in raw meats. Food Res Int 67:12–18
31. Yalcin H, Ozturk I, Karaman S, Kisi O, Sagdic O, Kayacier A (2011) Prediction of effect of natural antioxidant compounds on hazelnut oil oxidation by adaptive neuro-fuzzy inference system and artificial neural network. J Food Sci 76(4):112–120
32. Hubert M, Ousseeuw P, Branden K (2005) ROBPCA: a new approach to robust principal component analysis. Technometrics 47(1):64–79
33. Naganathan GK, Grimes LM, Subbiah J, Calkins CR, Samal A, Meyer GE (2008) Visible/near-infrared hyperspectral imaging for beef tenderness prediction. Comput Electron Agric 64:225–233
34. Argyri A, Panagou EZ, Tarantilis P, Polysiou M, Nychas G-JE (2010) Rapid qualitative and quantitative detection of beef fillets spoilage based on Fourier transform infrared spectroscopy data and artificial neural networks. Sens Actuators, B 145:146–154
35. Kodogiannis VS, Pachidis T, Kontogianni E (2014) An intelligent based decision support system for the detection of meat spoilage. Eng Appl Artif Intell 34:23–36
36. Alshejari A, Kodogiannis VS, Petrounias I (2015) An adaptive neuro-fuzzy model for the detection of meat spoilage using multispectral images. In: 2015 IEEE international conference on fuzzy systems (FUZZ-IEEE), Istanbul, Turkey, pp 1–7
37. De Jong S (1993) SIMPLS: an alternative approach to partial least squares regression. Chemom Intell Lab Syst 18(3):251–263
38. Li D-C, Hsu H-C, Tsai T-I, Lu T-J, Hu SC (2007) A new method to help diagnose cancers for small sample size. Expert Syst Appl 33:420–424